SEISMIC RESPONSE OF BUILDINGS DURING EARTHQUAKES: EXPERIMENTAL RESULTS FROM STRONG MOTION DATA

P.- Y. Bard [1], H. Afra[2] and P. Argoul[3]

ABSTRACT

The kinematic behaviour of 25 "standard" buildings is derived from an analysis of 29 accelerometric record sets obtained by the California Strong Motion Instrumentation Program during recent earthquakes. Measurements of the main natural frequencies, modal shapes, and corresponding dampings, are obtained by means of a multi-sensor, multi-degree of freedom linear system identification technique, while various spectral techniques (Fourier spectral ratios, coherence analysis) provide reliable, quantitative estimates of the amount of torsional and rocking motions (where there is adequate instrumentation). The results obtained are presented and discussed in connection with the geometrical and structural characteristics of the buildings.

I. INTRODUCTION

Over the last 15 to 20 years, many buildings have been extensively instrumented with accelerometric sensors so as to record their motion during moderate to strong earthquakes, especially in California by means of the structural strong motion networks of the California Strong Motion. Instrumentation Program (CSMIP), and, though to a lesser extent, of the United States Geological Survey. As a consequence of various moderate-size (e.g., Morgan Hill, 1984 or whittier Narrows, 1987) or large (Loma Prieta, 1989) shocks, numerous (over 50) structural records have therefore been obtained during the last decade.

Despite the extremely high quality of most of these data, very few attempts have been made to analyse and compare them with predictions obtained with more or leis sophisticated models, or formulae recommended in various building codes. The present study is an analysis of a selected but important set of the available SMIP structural recordings (i.e. those that have been digitized and disseminated). After a short presentation of this data set in section II, section III is devoted to a brief outline of the various mathematical techniques used to analyse these data in view of determining the vibration characteristics of the corresponding buildings, comprising i) a multi-sensor linear identification scheme providing reliable measurements of their modal parameters(natural frequencies, modal damping and modal shapes), and ii) spectral techniques for estimating torsional and rocking motions (whenever possible).

1 Research engineer, LCPC Paris and LGIT Grenoble, IRIGM, BP 53x, 38041 Grenoble Cedex, France

[2] Ph.D. Student, LCPC - Service Mécanique - La Courtine, 93167 Noisy-le-Grand, France

[3] Research engineer, LCPC - Service Mécanique - La Courtine, 93167 Noisy-le-Grand, France

the results obtained by the application of each of these analysis methods to the entire data set are then presented and discussed in sections IV (modal parameters), V (torsional motion) and VI (rocking motion). Conclusions are summarized in section VII, which also briefly discusses the relevance of their results for the special case of Mexico City.

II. DATA

For this study, we selected within the available SMIP digitized data 29 record sets, corresponding to 25 buildings 2 to 21 stories high (4 buildings were shaken by 2 earthquakes), and peak accelerations within the building ranging between .08 g and 1.24 g. This building set consists of 13 reinforced concrete buildings (labeled CI to C13), 7 steel buildings (SI to S7), 4 composite (concrete/steel) structures (CSI to CS4), and 1 masonry building (M1). Within the concrete buildings, 6' have a shear wall lateral resistance system (C1 to C6), 6 have a moment resisting frame (C7 to C11 and C13), and 1 has both shear walls and moment resisting frame (C12). It must be emphasized that, since SMIP philosophy is to instrument common and regular buildings, all the buildings dealt with in this study may be considered as representative of "average" buildings in California, and results of the present analysis should not be biased by special "extraordinary" structural behaviours.

The gross characteristics of these buildings, as given by CSMIP, are listed in Tables 1 through 4, respectively, together with those of the corresponding records. These tables point out that most of data come from low to medium rise buildings, and correspond to moderate shaking (peak structural acceleration lower than 0.3 g); there exist, however, a few very large acceleration levels (up to 1.24 g). Nevertheless, none of the selected buildings suffered structural damage during the corresponding earthquakes, so that we are sure that no irreversible, non-linear behaviour will alter the analysis. A more detailed description of these buildings may be found in the relevant SMIP processed data reports, listed in the reference section. (Porter et al., 1979; Huang et al., 1985; Shakal et al., 1987).

As a consequence of the differences in construction material and lateral resistance system, five different "building classes" may be identified, labelled CI, CII, S, CS, and M:

- CI corresponds to vibrations involving concrete shear walls, and thus consists of longitudinal and transverse vibrations of buildings C1 to C6, and transverse vibrations of building C12.

- CII corresponds to vibrations involving concrete moment resisting frames, and thus consists of longitudinal and transverse vibrations of buildings C7 to C11 and C13, and longitudinal vibrations of building C12.

- S corresponds to vibrations involving steel frames, and thus consists of longitudinal and transverse vibrations of buildings S1 to S7.

- CS corresponds to vibrations involving composite steel/concrete structures, and thus consists of longitudinal and transverse vibrations of buildings CS1 to CS4,

- M corresponds to vibrations involving masonry structures.

In the remainder of this paper, results will be grouped for each "building class" so as to investigate whether some particular characteristics may be identified for each of them.

III. DATA ANALYSIS TECHNIQUES

III.1 Linear identification scheme

For each of these 29 record sets, we applied the system identification technique described in more detail in Afra et al., 1990. Basically, this method minimizes in a least-square sense the difference, measured in the time domain, between an MDOF linear model and the actual acceleration records. The minimization follows the scheme proposed by Beck and Jennings (1980), with a significant improvement however: it considers simultaneously all the transverse (resp. longitudinal) sensors located in a given structure, thus forcing the frequencies and modal dampings to be the same for all these sensors (the participation factors, initial velocities and initial displacements remaining free, of course, for each sensor).

In other words, if there exist, for a given horizontal direction, N_p sensors above the level, each vibration mode r along this direction is described by $N_r = 2 + 3\,N_p$ parameters, *i.e.* its frequency f_r, its damping ζ_r, and the N_p groups xx xxxxxxxxxxxxxxxxx where: xxxxx is the participation factor at node i for mode r, xxxx is the initial displacement at mode r, and xxxx is the initial velocity at node i for mode r. (These latter values cannot be set equal to zero since recordings are made with CRA-1 analog-optical-instruments, which do not have any pre-event memory.)

TABLE 1: DATA FOR CONCRETE BUILDINGS

	Building							Records		
		Structural characteristics			Dimensions					
Id	Name and location	Lateral resistance system	Foundation	Story number	h (m)	L (m)	l (m)	Event	A_{max} ground (g)	A_{max} struct. (g)
C1	UCSB North Hall (Goleta)	Shear Walls	Caissons, tie beams and slab	3/0	10.1	73.2	10.4	SB78	0.41	0.99
C2	Telephone Bldg (Watsonville)	Shear Walls	Spread flags	4/0	20.2	22.7	21.5	MH84 LP89	0.11 0.68	0.33 1.24
C3	Freitas Bldg (Santa Barbara)	Exterior shear walls	Spread flags and caissons	4/1	16.2	41.9	33.3	SB78	0.22	0.67
C4	Engng Bldg E1, Cal. State Col. (Long Beach)	Shear walls	Conc. piles	5/1	21.5	62.5	24.7	WN87	0.10	0.36
C5	Pacific Manor (Burbank)	Shear walls	Conc. caissons	10/0	28.8	65.6	22.9	WN87	0.22	0.54
C6	Town Park Towers Apartment Bldg (San Jose)	Shear walls	Conc. piles	10/0	29.3	63.9	19.4	MH84 ML86	0.06 0.03	0.22 0.12
C7	First Federal Savings Bank (Pomona)	Perimeter ductile MR frame	Conc. piles	2/1	9.1 + 3.2	36.6	30.5	WN87	0.05	0.16
C8	Sears Warehouse (Los Angeles)	Ductile RC perimeter frame	Spread flags	5/1	36.3 + 5.9	109.7	85.3	WN87	0.18	0.28
C9	Holiday Inn (Van Nuys)	MR frame	Conc. piles	7/0	20.0	46.0	19.2	WN87	0.17	0.30
C10	Hollywood Storage Bldg (Los Angeles)	RC frame	Conc. piles	14/1	45.3 + 2.7	66.1	15.5	WN87	0.12	0.21
C11	Sheraton-Universal Hotel (North Hollywood)	Ductile MR frame	Spread flags	20/1	51.5 + 2.5	58.1	17.7	WN87	0.10	0.22
C12	Great Western Savings & Loan Bldg (San Jose)	T: End shear walls L: MR frame	RC mat	10/1	37.8 + 5.2	57.9	25.0	MH84 ML86	0.06 0.04	0.22 0.08
C13	Union Bank Bldg (Sherman Oaks)	MR frame (above grnd) Shear walls (below)	Conc. piles	13/2	50.0 + 6.2	58.8	22.9	WN87	0.15	0.28

Comment: SB78 – Santa Barbara, 8/13/78 (M_L=5.1); MH84 – Morgan Hill, 4/24/84 (M_L=6.2); BH86 – Berkeley Hills, 5/29/86 (M_L=4.0); ML86 – Mount Lewis, 3/31/86 (M_L=5.8); WN87 – Whittier Narrows, 10/1/87 (M_L=5.9); LP89 – Loma Prieta, 10/17/89 (M_s=7.1).

TABLE 2: DATA FOR STEEL BUILDINGS

Building								Records		
		Structural characteristics			Dimensions					
Id	Name and location	Lateral resistance system	Foundation	Story number	h (m)	L (m)	l (m)	Event	A_{max} ground (g)	A_{max} struct. (g)
S1	Alta Bates Hospital (Berkeley)	Braced steel frames Conc. floors & roof	Conc. mat	2/1	7.7 + 4.7	42.9	38.1	BH86	0.08	0.12
S2	Sunwest Office Bldg (San Bernardino)	Steel MR frame Plywood & conc. floors	Spread ftngs w/grade beams	3/0	12.8	43.9	40.2	WN87	0.03	0.08
S3	Kaiser Medical Center (South San Francisco)	MR steel frame	Spread ftngs on piles	4/0	16.0	63.7	32.6	MH84	0.03	0.26
S4	Cal. Federal Savings Bldg (Burbank)	MR frames in perimeter walls	Conc. caissons	6/0	25.1	36.6	36.6	WN87	0.23	0.29
S5	Harbor Adm. Bldg (Long Beach)	Steel frame	Column ftngs on piles	7/0	27.7 + 4.0	67.1	22.9	WN87	0.07	0.12
S6	Santa Clara County Office Bldg (San Jose)	MR frames in perimeter walls	Conc. mat	13/0	64.2	50.9	50.9	MH84	0.04	0.17
								ML86	0.04	0.32
S7	City Hall (Long Beach)	MR frame	Spread ftngs & bell caissons	15/1	82.6 + 5.2	32.3	32.3	WN87	0.06	0.08

TABLE 3: DATA FOR COMPOSITE (STEEL & CONCRETE) BUILDINGS

Building								Records		
		Structural characteristics			Dimensions					
Id	Name and location	Lateral resistance system	Foundation	Story number	h (m)	L (m)	l (m)	Event	A_{max} ground (g)	A_{max} struct. (g)
CS1	Century City Bullock Store (Los Angeles)	Conc. shear walls (n=2-0) Steel perimeter braced frame (n>0)	Spread ftngs & bell caissons	3/2	15.2 + 6.9	73.5	66.8	WN87	0.06	0.18
CS2	Olive View Medical Center (Sylmar)	Conc. shear walls (n=1-3) Steel perim. shear walls (n>3)	Spread ftngs	6/0	29.3	137.8	92.0	WN87	0.06	0.20
CS3	UCLA Math. Science Bldg (Los Angeles)	Thick shear wall (n=1-3) MR steel frame (n>3)	?	7/0	28.8	18.3	14.6	WN87	0.05	0.14
CS4	CSULA Admin. Bldg (Los Angeles)	Conc./steel columns (n=1-2) Conc. shear walls (n>2)	Spread ftngs & bell caissons	8/1	36.6 + 3.7	46.9	19.3	WN87	0.39	0.53

TABLE 4: DATA FOR MASONRY BUILDINGS

Building								Records		
		Structural characteristics			Dimensions					
Id	Name and location	Lateral resistance system	Foundation	Story number	h (m)	L (m)	l (m)	Event	A_{max} ground (g)	A_{max} struct. (g)
M1	Medical Office Bldg (Lancaster)	Block masonry shear walls Plywood floor & roof diaphragms	Conc. piers & grade beams	3/0	12.8	39.3	21.3	WN87	0.06	0.19

If only one mode is to be identified, the identification technique looks for the N o parameters f_0, ζ_0, f_0, ζ_0, $((\phi_0^i, d_0^i, v_0^i), i=1,N_p)$ defining the set equations:

$$\ddot{y}_i + 2\zeta_0\omega_0\dot{y}_i + \omega_0^2 y_i = \phi_0^i \ddot{x}_b \quad \text{for} \quad i=1,N_p, \tag{1}$$

so that the following "error function" E is minimized:

$$E = K \sum_{i=1}^{i=N_p} \left[\int_0^{T_d} (\ddot{x}_i(t) - \ddot{y}_i(t))^2 \, dt \right] \tag{2}$$

where: $\ddot{x}_i$ is the recorded relative acceleration of node i with respect to base level, characterized by $\ddot{x}_b$,

$\ddot{y}_i$ is the relative acceleration $\ddot{y}_i^0$ computed with the identified SDOF model characterized by parameters $(f_0, \zeta_0, \phi_0^i, d_0^i, v_0^i)$ (equation (1)),

K is a normalization factor,

$$K = \left\{ \sum_{i=1}^{i=N_p} \left[\int_0^{T_d} \ddot{x}_i(t)^2 dt \right] \right\}^{-1} \tag{3}$$

T_d is the total time duration of the records (usually between 20 an 40 s, in some cases up to 80 s),

If more than one mode is to be identified, an iterative procedure is used, starting with the identification of the first mode, and taking in the error function (2), for each additional mode m, the computed relative motion y_i equal to

$$y_i = \sum_{r=0}^{r=m} y_i^r.$$

Other error functions than those presented above are possible. Some of them were tried, but the corresponding results did not show any significant differences, especially for the first modes. It was observed, however, that the identification of higher modes was better with an error measurement based on the relative accelerations, than with an error based on the relative displacements, as often proposed.

The input motion for the SDOF linear systems is taken to be equal to the measured based motion x_b (which implies neglecting any translational soil structure interaction); when more than one sensor exists at the base level (which is often the case for the transverse direction), the input motion is taken to be equal to the mean of these sensors. As an example, for the building shown in Figure 1, identification of longitudinal modes involves sensors 5, 9 and 10, with input motion provided by sensor 13, while the identification of transverse modes considers sensors 3, 4, 6 and 8, with the input motion given by the mean of sensors 11 and 12.

A more detailed discussion of the limitations of this method may be found in Afra et al. (1990); in particular, it does not take into account any coupling between the longitudinal and transverse modes, and it also does not pay any attention to the non-linear behaviour of these structures, which may be significant when shaken by moderate to strong base motion. These limitations should be reflected, however, in the residual error E: a moderate value for E, i.e. less than 20%, is therefore a good a posteriori justification of the use of this linear identification technique: it is shown in section IV that this requirement was met in most cases for the present data set.

In the present identification study, we did not estimate the precision of the results, especially regarding modal frequencies and damping. This precision study is now under way (based on the sensitivity of the error function on the various parameters, and using the Hessian matrix), and the preliminary results show that the precision on the fundamental frequency is very good, certainly not exceeding 5% while the precision on the estimated damping is significantly lower: though additional work is needed to quantify precisely this uncertainty, we estimate it to be around 20% to 30%.

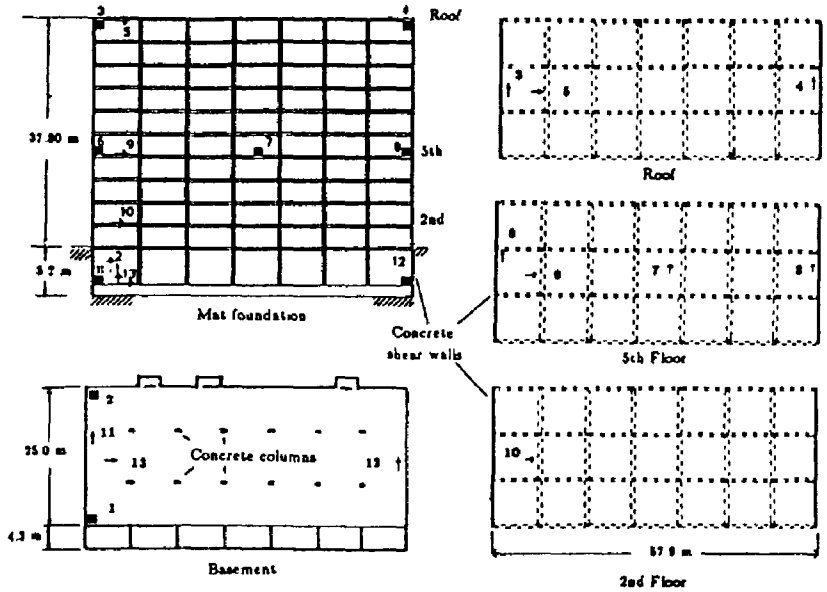

Figure 1: ***Structural plan and instrumentation scheme for one sample building: C12 (after CSMIP, [2])***

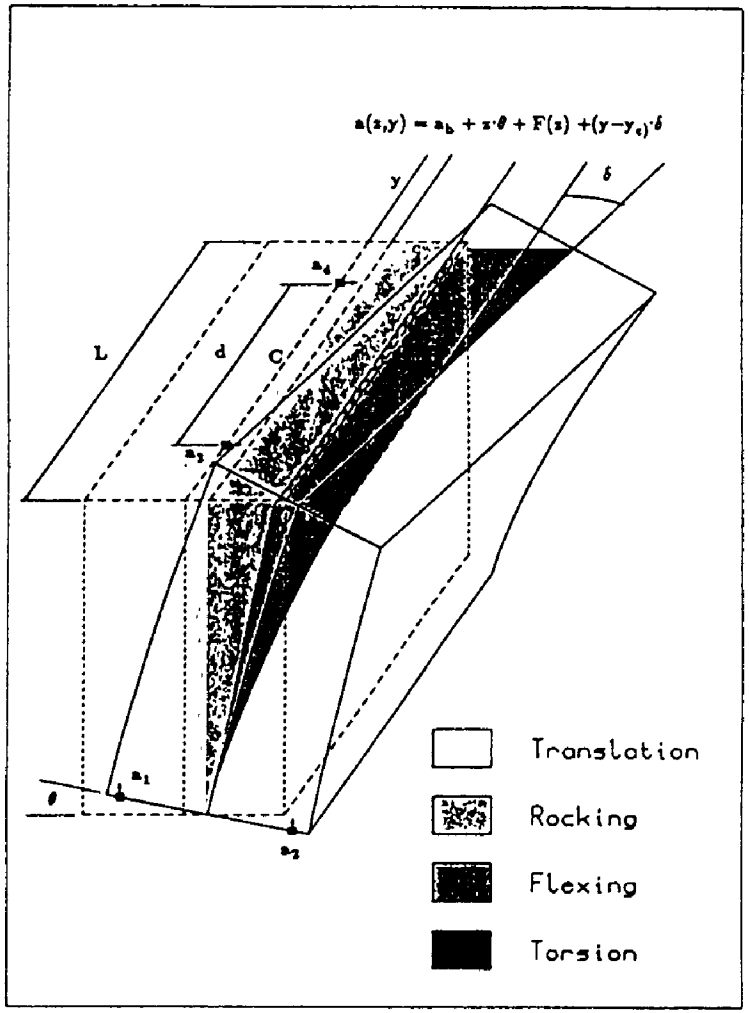

Figure 2: *Estimation of rocking and torsional motions for a building instrumented with two vertical sensors at the base level and two transverse sensors at roof level.*

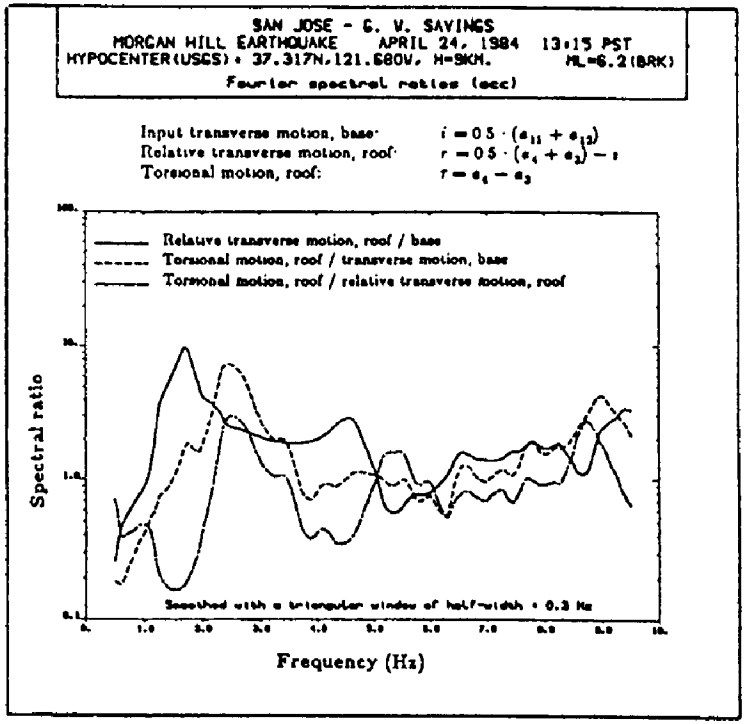

Figure 3: *An example of smoothed spectral ratios allowing the quantification of torsional motion. The example building is building C12 displayed in Figure 1; sensors 3 and 4 are transverse sensors at the roof level, while sensors 11 and 12 are transverse sensors at the base level.*

III.2 Determination of torsional motion

All 25 buildings are instrumented with several pairs of transverse sensors located on different floors (roof, basement and one or more intermediate levels, see Figure 1). Differences between two transverse sensors located on the same floor thus provide an estimation of the torsional motion, as illustrated in Figure 2.

In the present study, the torsional motion was therefore analyzed with the following technique, illustrated on the example of the building displayed in Figure 1:

a) computing the average input transverse motion: $i(t) = 0.5\ (a_{11}(t) + a_{12}(t))$, the average roof relative transverse motion: $r(t) = 0.5\ (a_4(t) + a_3(t)) - i(t)$, and the roof torsional motion $\tau(t) = a_4(t) - a_3(t) = (Y_4 - Y_3) \cdot \sin\delta(t)$ (see Figure 2).

b) computing their Fourier transforms, over the whole signal duration, and their modulus $I(f)$, $R(f)$ and $T(f)$.

c) computing the smoothed spectral ratios $RI(f) = R(f) / I(f)$, $TI(f) = T(f) / I(f)$, and $TR(f) = TR(f) / R(f)$.

Peaks on TI(f) allow us to identify the frequencies f_i^T of the torsional modes (as well as peaks on RI(f) must correspond to the transverse frequencies f_i^T, found using MDOF system identification techniques), and the corresponding values $TR(f_i^T)$, and $TR(f_i^T)$, provide a quantitative estimate of the proportion of torsional motion in the transverse motion, at the resonant frequencies (transverse and torsional). Examples of such smoothed spectral ratios, computed for C12 building, are depicted in Figure 3.

Very often, however, the two sensors are not located at the end walls of the building (separated by distance L, but at a closer distance d. In order to compare data from different buildings, we therefore estimated the torsional motion between the end walls by assuming that the roof is rigid rotating block (see Figure 2), which leads to the formula:

$$Tor_L(f_i) = 0.5\ TR(f_i) \cdot L/d \qquad (4)$$

This rigid block assumption may not be valid for some modes, for instance diaphragm vibrations; we used it, however, only for fundamental transverse and torsional modes ($i=0$), which should not be influenced by these modes, generally occurring at higher frequencies.

III.3 Rocking motion

Some buildings, such as the example building C12 in Figure 1, are instrumented with 2 or more vertical sensors at the base level. On the assumption of a rigid base, their rocking motion, characterized by the angle θ (Figure 2), may thus be estimated from the difference between the

respective vertical motions on each side of the foundation. (If the base is flexible, the actual rocking motion of the building should be larger than θ (t) , as found in Luco et. al. (1987): in the present study, we always assumed a rigid base, and our results are therefore lower bound estimates of the rocking motion).

We followed the analysis procedure detailed in Bard (1988), which, for the building displayed in Figure 1, may be summarized as follows:

a) estimating the rocking angle $\theta(t)$

$$\theta(t) = (a_2(t) - a_1(t))/l$$

where a_i (t) is the acceleration history at (vertical) sensor i, and l is the distance to the two vertical sensors.

b) comparing this rocking motion with the mean total transverse motion relative to the base, for instance at the roof level:

$$T_{roof}(t) = 0.5 \times \left\{ a_3(t) + a_4(t) - a_{11}(t) - a_{12}(t) \right\},$$

In most cases, θ and T_{roof} proved to have very similar signal shapes, as displayed on Figure 4 for building C12 of Figure 1. This similarity was therefore quantified by means of the coherence between both signals, computed over their whole duration (40 s), and smoothed with a triangular running window having a 0.6 Hz half-width, as illustrated in Figure 5. Despite this broad smoothing window, the coherence very often reaches very high values (larger than 0.99) for frequencies around the fundamental transverse mode.

As, in this frequency band, the spectral ratio between both signals is very flat (Figure 5), reliable and meaningful measurements of the percentage P of rocking (R) in the transverse relative motion (T) are possible.

$$P = R_{roof}(f_0) \,/\, T_{roof}(f_0) \qquad (5)$$

where $R_{roof}(f) = h \cdot (2\pi f)^2 \cdot \Theta(f)$, $\Theta(f)$ is the Fourier transform of $\theta(t)$, and f_0 is the fundamental transverse frequency.

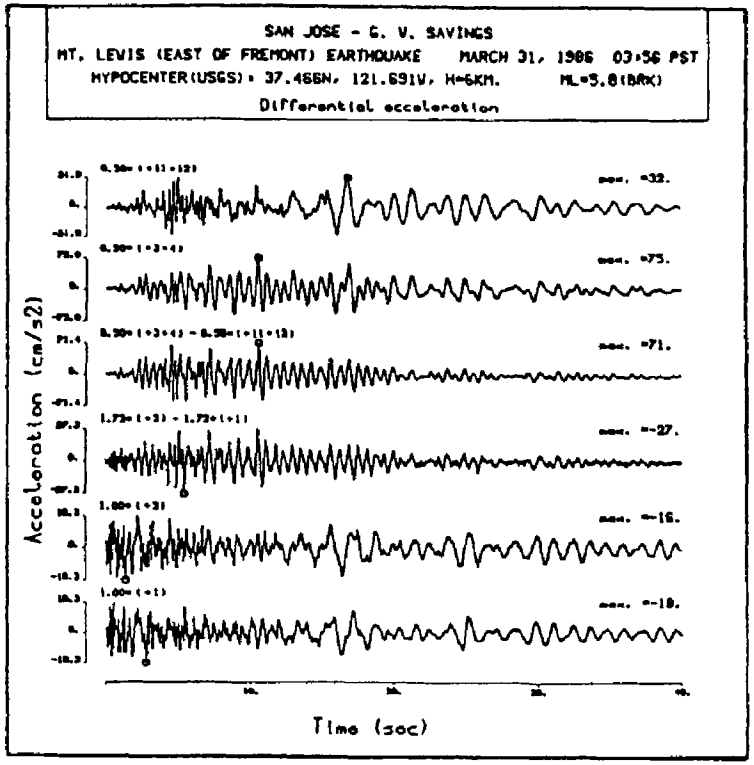

Figure 4: *An example of rocking motion for building C12 (see Figure 1). Original (processed) acceleration traces recorded by the vertical sensors (2 bottom traces) and the transverse sensors at base and roof levels (2 top traces). The two intermediate traces display a comparison between the computed rocking motion at roof level (3rd trace from bottom), and the transverse motion of the roof relative to the base (4th from bottom). The amplitude scale is different for each trace, so as to highlight the signal similarities.*

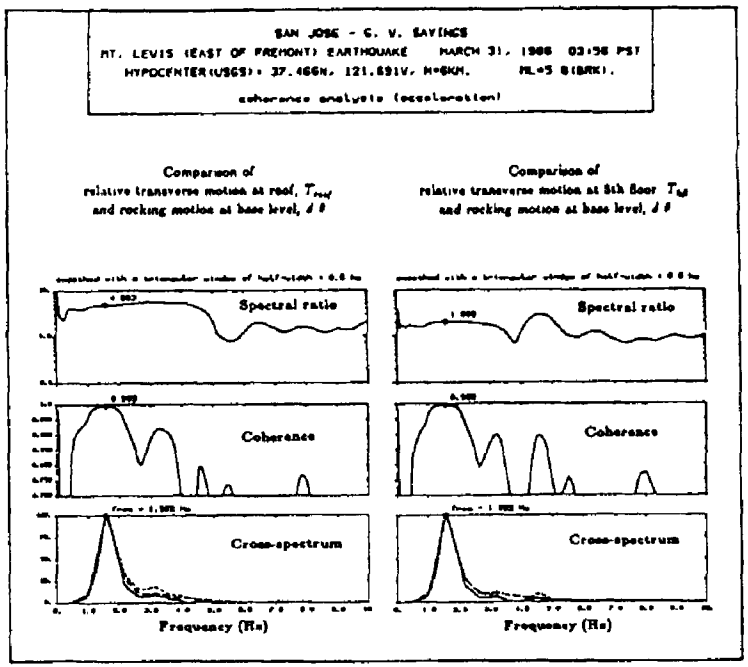

Figure 5: *Normalized cross-spectrum, coherence and spectral ratios between the relative transverse motion at roof (left) and at 5th floor (right) levels and the corresponding rocking motion. See text for further explanations.*

IV. ANALYSIS OF THE MODAL PARAMETERS

Tables 5 through 8 display the values obtained for the frequencies and dampings of the concrete (5), steel (6), composite (7), and masonry (8) buildings, along the two horizontal directions (longitudinal, *i.e.* along the longest horizontal dimension, and transverse). Also displayed in these tables, are the error levels considering one, two, ...N_m modes. The number of identified modes N_m, depends on the building: it was limited to the modest that contribute significantly to the response, i.e. those modes the consideration of which induces a significant decrease in the residual error E.

TABLE 5. IDENTIFIED PARAMETERS FOR CONCRETE BUILDINGS

Building characteristics					First mode			Second mode			Third mode			Event	
Id	Component	h (m)	D1 (m)	D2 (m)	f_0 (Hz)	ς_0 (%)	E_0 (%)	f_1 (Hz)	ς_1 (%)	E_1 (%)	f_2 (Hz)	ς_2 (%)	E_2 (%)		A_{max} (g)
C1	L	10.1	73 2	10.4	4.51	12.7	21.7	0.	0.	0.	0.	0.	0.	SB78	0.99
	T	10.1	10.4	73.2	3.23	9.2	31.9	0.	0.	0.	0.	0.	0.	SB78	0.99
C2.1	L	20.2	22.7	21.5	3.61	6.2	9.7	0.	0.	0.	0.	0.	0	MH84	0.33
	T	20.2	21.5	22.7	4.78	14.9	20.2	0.	0	0	0.	0.	0.	MH84	0.33
C2 2	L	20.2	22.7	21.5	2.70	8.1	17.5	0.	0.	0.	0.	0.	0.	LP89	1.24
	T	20.2	21.5	22.7	3.75	15.9	30.4	0.	0.	0.	0.	0.	0.	LP89	1.24
	T	20.2	21.5	22.7	4.78	14.9	20.2	0.	0.	0.	0.	0.	0.	MH84	1.24
C3	L	16.2	41.9	33.3	1.80	13.2	22.6	4.99	12.0	17.4	0.	0.	0.	SB78	0.67
	T	16.2	33.3	41.9	2.51	10.6	40.2	3.51	1.6	36.5	6.12	30.1	23.1	SB78	0.67
C4	L	21.5	62.5	24.7	5 58	12.2	12 8	0.	0.	0.	0.	0.	0.	WN87	0 36
	T	21.5	24.7	62.5	2.99	4.6	16.7	0.	0.	0.	0.	0.	0.	WN87	0.36
C5	L	26.8	65 5	22.9	1 94	7.9	57.6	8.34	16.7	44.9	0.	0.	0.	WN87	0 54
	T	26.8	22.9	65.5	2.17	5.1	30.5	8.25	10.3	20.6	0.	0.	0.	WN87	0.54
C6	L	29.3	63 9	19 4	1.61	7.7	29.2	5.63	11.6	27.7	0.	0.	0.	MH84	0 22
	L				1.58	3.6	6.3	5.54	8.9	4.2	0.	0.	0.	ML86	0.12
	T	29.3	19 4	63.9	2.35	5.3	12.4	0.	0.	0.	0.	0.	0.	MH84	0.22
	T				2 42	3.7	16.5	0.	0.	0.	0.	0.	0.	ML86	0.12
C12	T	37.8	25.0	57.9	1.62	6.6	34.7	0.	0.	0.	0.	0.	0.	MH84	0.22
	T				1 63	3.0	10 4	0.	0.	0.	0.	0.	0.	ML86	0.08
C7	L	9.1	36.6	30.5	3 71	7 9	12.2	0.	0.	0.	0.	0.	0.	WN87	0.16
	T	9 1	30.5	36.6	3.39	6.4	50.5	0.	0.	0.	0.	0.	0.	WN87	0.16
C8	L	36 3	109.7	85.3	0.75	6 5	47 1	2.26	7.8	19.7	5.59	20.6	17.4	WN87	0.28
	T	36.3	85.3	109.7	0.70	4.0	36.7	2.15	11.6	19.8	4.03	12.2	16.8	WN87	0.28
C9	L	20.0	46.0	19.2	0.97	10.1	25.7	3.42	10.4	8.9	0.	0.	0	WN87	0.20
	T	20 0	19.2	46 0	0.86	19.6	53 1	3 16	16.8	17.2	0.	0.	0	WN87	0.20
C10	L	45.3	66.1	15.5	1.58	10.7	22.4	5.38	11.8	11.8	0	0.	0.	WN87	0.21
	T	45 3	15.5	66.1	0.54	9.4	51 3	2.02	9.6	32.0	3.47	8.5	25.8	WN87	0.21
C11	L	51 5	56.1	17.7	0.46	10.6	62 0	1.56	12.2	49 2	3 07	10.5	31.2	WN87	0.22
	T	51.5	17.7	56.1	0.55	6.4	69.6	1.69	9.5	42.8	2.73	7.6	31 8	WN87	0.22
C12	L	37 8	57.9	25.0	1.09	4.0	22.7	3.75	4.5	15 0	0.	0.	0.	MH84	0 22
	L				1.10	2.9	11 2	3.52	3 9	2.7	0	0.	0.	ML86	0.08
C13	L	50.0	58.8	22.2	0.44	5.7	31.5	1.52	4.2	23.5	2 58	7.8	9 2	WN87	0.28
	T	50.0	22.2	58.8	0.40	2.8	42.8	1.38	2.4	40.9	2.40	5.6	20 5	WN87	0.28

TABLE 6: IDENTIFIED PARAMETERS FOR STEEL BUILDINGS

Building characteristics					First mode			Second mode			Third mode			Event	
Id	Component	h (m)	D1 (m)	D2 (m)	f_0 (Hz)	ς_0 (%)	E_0 (%)	f_1 (Hz)	ς_1 (%)	E_1 (%)	f_2 (Hz)	ς_2 (%)	E_2 (%)		A_{max} (g)
S1	L	7.7	42 9	38.1	3.18	4.0	28.8	0.	0.	0.	0.	0.	0.	BH86	0 12
	T	7.7	38.1	42 9	3.09	2.7	31.6	4.85	7.7	24.6	0.	0.	0.	BH86	0 12
S2	L	12 8	43.9	40.2	2 16	7.5	15 7	6.00	13 7	11 7	0.	0.	0.	WN87	0.08
	T	12.8	40.2	43 9	2.12	5.5	29.0	5 63	27 2	26.7	0.	0.	0.	WN87	0.08
S3	L	16.0	63.7	32 6	1.79	5.8	11 9	5.52	7.5	10.5	0.	0	0.	MH84	0.26
	T	16.0	32 6	63.7	1.79	3.6	10 5	0.	0.	0	0.	0	0.	MH84	0 26
S4	L	25.1	36 6	36.6	0.78	2.9	42.1	2.32	6.0	7.5	4.31	17 0	4.9	WN87	0.29
	T	25.1	36.6	36.6	0.80	4.9	38.4	2.39	7.5	12.0	4.43	13.2	7.8	WN87	0.29
S5s	L	27.7	67.1	22.9	0.88	6.4	10.4	3.17	11.1	9.3	0.	0.	0.	WN87	0.12
S5s	T	27.7	22.9	67.1	0.72	4.5	17.7	2.26	5.4	8.4	0.	0.	0.	WN87	0.12
S5n	L	27.7	67.1	22.9	0.89	6.5	10.8	3.14	8.0	9.8	0.	0.	0.	WN87	0 12
S5n	T	27.7	22 9	67.1	0.71	6.5	21.3	2.25	6.7	14.2	0.	0.	0.	WN87	0.12
S6	L	64.2	50.9	50.9	0.48	3.0	16.7	1.40	3.9	5.9	0.	0.	0.	MH84	0.17
	L	64.2	50.9	50.9	0.48	2.4	49.5	1.37	3.2	42.6	0.	0.	0.	ML86	0.32
	T	64.2	50.9	50.9	0.50	1 3	27.3	1.45	4.6	11.9	2.42	5.6	10.7	MH84	0.17
	T	64.2	50 9	50.9	0 48	2.2	4.4	1.42	4.5	3.9	0.	0.	0.	ML86	0.32
S7	L	82.6	32 3	32.3	0.18?	47.9?	60.6?	0.86	4.8	33.2	1.58	9.4	19.9	WN87	0.08
	T	82.6	32.3	32.3	0.28	3.0	69.5	0.84	5.6	22.8	1.60	14.1	14.6	WN87	0.08

TABLE 7: IDENTIFIED PARAMETERS FOR COMPOSITE BUILDINGS

Building characteristics					First mode			Second mode			Third mode			Event	
Id	Component	h (m)	D1 (m)	D2 (m)	f_0 (Hz)	ς_0 (%)	E_0 (%)	f_1 (Hz)	ς_1 (%)	E_1 (%)	f_2 (Hz)	ς_2 (%)	E_2 (%)		A_{max} (g)
CS1	L	15.2	73.5	66.8	2 20	6.0	23.9	4.92	9.3	9.8	0.	0.	0.	WN87	0.18
	T	15.2	66.8	73.5	2.55	8.1	31.9	5.44	9.5	16.3	0.	0.	0.	WN87	0.18
CS2	L	29.3	137.8	92.0	3.58	8.6	54.4	0.	0.	0.	0.	0.	0.	WN87	0.20
	T	29.3	92.0	137.8	3 33	5.0	36.1	7.32	7.8	24.9	0.	0.	0.	WN87	0.20
CS3	L	28.8	18.3	14.6	1.22	9.5	27.0	0.	0.	0.	0.	0.	0.	WN87	0.14
	T	28.8	14.6	18.3	1.64	17 0	39.1	4.64	11.0	34.8	0.	0.	0.	WN87	0.14
CS4	L	36.6	46.9	19.3	0.65	6.5	26.9	1.87	9.1	5.7	4.72	4.1	4.8	WN87	0.53
	T	36.6	19.3	46.9	0.66	7.6	8.4	2.04	6.0	33.9	0.	0.	0.	WN87	0.53

TABLE 8: IDENTIFIED PARAMETERS FOR MASONRY BUILDINGS

Building characteristics					First mode			Second mode			Third mode			Event	
Id	Component	h (m)	D1 (m)	D2 (m)	f_0 (Hz)	ς_0 (%)	E_0 (%)	f_1 (Hz)	ς_1 (%)	E_1 (%)	f_2 (Hz)	ς_2 (%)	E_2 (%)		A_{max} (g)
M1	L	12 6	39.3	21 3	5.32	13.3	47.5	11.15	17.8	30.9	0.	0.	0.	WN87	0.19
	T	12.6	21 3	39.3	4.70	14.0	51.9	9.24	11.4	37.7	0.	0.	0.	WN87	0.19

IV.1 Error analysis

The distribution of these residual errors is displayed in Figure 6 as a function of the "building class", as defined in section II. These errors were also analyzed in connection with various possible "explaining parameters", namely the peak structural acceleration A_{max} (in relation with non-linearities), the building height, its horizontal dimension along the vibration direction, and its "elongation ratio" L/I: the results of this analysis are briefly summarized hereafter.

For the CI class, the mean (logarithmic) error for the 18 cases is around 18% which is satisfactory, but not excellent. The worst identification is found for the longitudinal vibrations of building C5, which corresponds to the most complicated shear wall structure Shakal et al. (1987). Also, there appears to be a relatively good correlation between the peak structural acceleration (cf Table 1) and the final error, therefore suggesting that this error comes, at least partly, from some kind of non-linear behaviour in these concrete structures; this is supported in particular by the error values found for the 3 buildings having experienced 2 earthquakes (C2, C6 and C12).

For the CII class (14 cases), the mean logarithmic error has about the same level (16%). The worst identification occurs for transverse vibrations of building C7, which will be shown in later section to be the building with the largest torsional motion, which may therefore alter the identification. For this class of buildings, there is no clear correlation between the error and the peak structural acceleration, nor with any other simple parameter.

For the S class (16 cases), the mean error is about 12%, which is both very satisfactory, and significantly smaller than for concrete buildings. The worst identification occurs for "longitudinal" vibrations of S6 building, when shaken by the Mount Lewis earthquake (while the error is much smaller when shaken by the Morgan Hill earthquake): once again, this large residual error corresponds to a large torsional motion (see section V). For this class of buildings, the residual error exhibits some correlation with two parameters: the building height and the peak structural acceleration. The latter correlation is unusual, however, since the error decreases with increasing acceleration: this observation, combined with the low value of the average error, allows us to suggest that most of these steel buildings behaved linearly during these earthquakes.

Finnaly, for the CS class (8 cases). the average error is about 21%, thus indicating that their behaviour is more complex than for "pure concrete" or "pure steel" buildings, as expected. Moreover, there does not appear to be any clear correlation between error and peak acceleration or any other simple parameter.

In other words, the proposed linear identification technique works very well for steel buildings, well for concrete buildings, and reasonably well for composite buildings; as there clear evidence of an error increasing with increasing acceleration only for shear wall concrete buildings, we attribute this variable "performance" of the identification technique mainly to the fact that steel buildings have in general the simplest and purest dynamic behaviour, while masonry and composite buildings have the most complex, with mode to mode coupling.

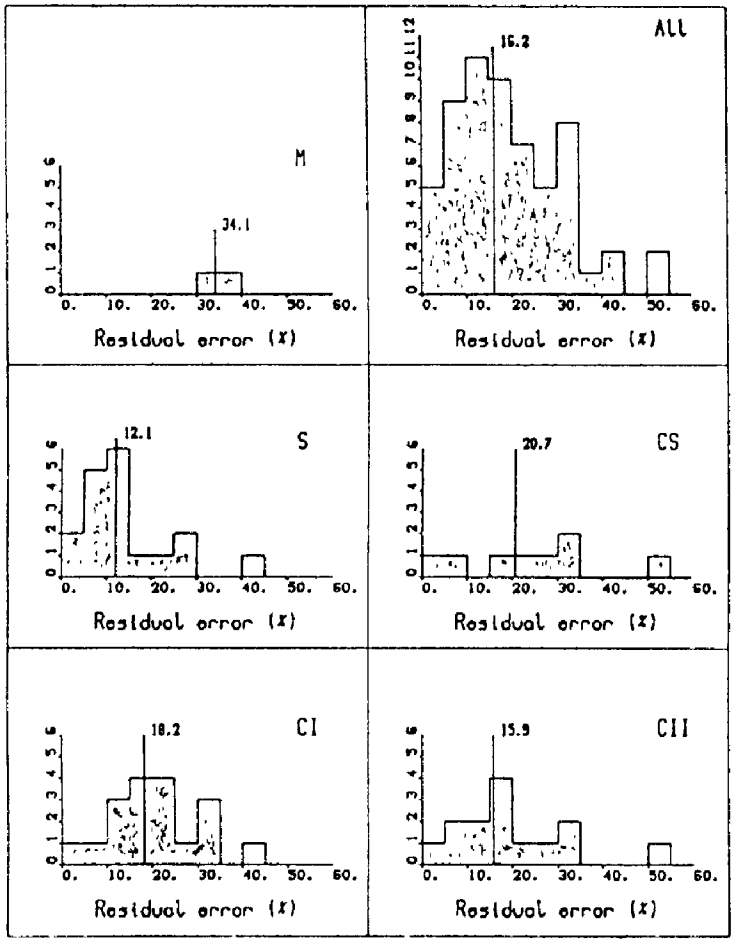

Figure 6: *Distribution of residual error for each building class and for the whole data set. All identifications are considered here, i e for the 29 accelerometric data sets, and, for each building, along each horizontal direction.*

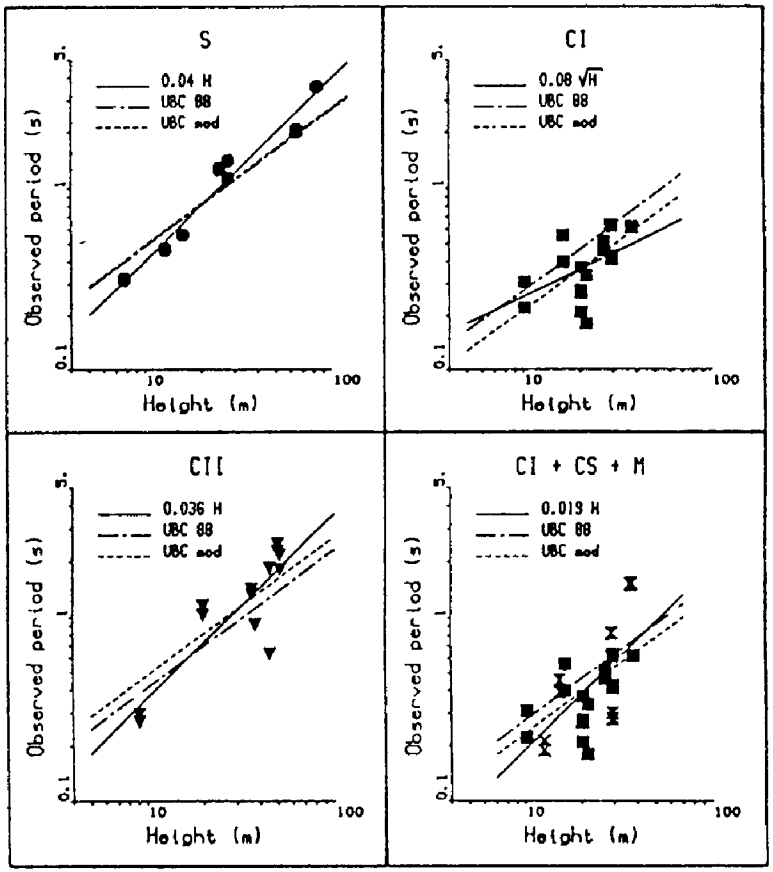

Figure 7: *Correlation between the fundamental period T_0 and building height, for the 4 different building classes. Dotted lines represent the original and modified UBC formulæ, while straight lines represent the formulæ proposed in this study (Tables 10).*

IV.2 Fundamental frequency

Very often, for simple buildings, this frequency is estimated roughly by means of simple formula proposed in earthquake regulations. Although there exist a large number of such formula, some are more extensively used than others, amongst which:

the ATC formula: $$T_0 = 0.09\ H\ /\ \sqrt{D} \qquad (6)$$

genneraly considered as valid only for rather stiff buildings, and recommended, under some limitations, in many countries

the UBC formulæ: $$T_0 = C\ H^{0.75} \qquad (7)$$

with C depending on the structural type: 0.085 for steel moment resisting frames (i.e., S class), 0.073 for reinforced concrete moment-resisting frames (CII class) and eccentric braced frames, and 0.049 for all other buildings (mixing of CI, CS and M class). (These values stand for geometrical dimensions H and D measured in meters).

In order to test these various formulae, we performed, for each of the main classes (CI, CII, S, CS) and also for mixed CI+CS+M (corresponding to the "all other buildings" category in UBC classification) and all buildings, a least-square regression fitting the dependance of $log f sub 0$ on $log H$ and $log D$. Other explaining variables were tried, but the corresponding fit improvements were not significant (considering the small extent of the data set), and therefore no other parameter was introduced. The results of such regression are summarized in Table 9, showing that the main parameter is, by far and for each class, the building height H; consideration of the horizontal dimension D significantly improves the fit only for steel buildings, for which the agreement is, however, already very good with H alone.

TABLE 9: DEPENDENCE OF f_0 ON H AND D

			$f_0 = \alpha_1 \times H^{\beta_1} \times D^{\gamma_1} \times 10^{\sigma_1}$				$f_0 = \alpha_2 \times H^{\beta_2} \times 10^{\sigma_2}$		
Building set	$\overline{f_0}$	σ_0	α_1	β_1	γ_1	σ_1	α_2	β_2	σ_2
CI	2 74	0.18	14.55	-0.55	0.00	0.15	14.62	-0.55	0 15
CII	0.89	0.30	13.91	-1.02	0.20	0.15	26.86	-0.99	0.16
S	1.11	0.32	7.49	-0.99	0.31	0.055	23.81	-0.98	0.067
CS	1.66	0.27	2.36	-0.63	0.45	0.18	46.15	-1.02	0.23
CI+CS+M	2.42	0.25	47.82	-0.97	0.00	0.19	47.82	-0.97	0.19
All	1.51	0.35	30.50	-1.07	0.11	0.22	44 63	-1.07	0.22

Comment: $\overline{f_0}$ is the mean value of the data set, and σ_0 is the corresponding (logarithmic) standard deviation.

Some interesting observations may be derived from these fits:

i)the best fit is obtained (by far) for the steel buildings data set, and within concrete buildings, the fit is much better for CII set (compare σ_0 and σ_1 in Table 9). This is related to the fact the residual error is minimal for steel buildings also, and points towards simpler behaviour of steel buildings, and, amongst concrete structures, of moment-resisting frame buildings.

ii) the data set for the CI category is limited to rather short periods: measured f_0 range between 1.5 and 5 6 Hz. This is too short a range to fit a satisfactory formula, and explains the large scatter in Figure 7. A better fit would certainly require incorporating of the actual resistance capacity of the shear walls (by means, for instance, of their section area), but this structural information was unavaible.

iii) the fundamental frequency depends much more on the type of lateral resistance structure (frame or shear walls) than on the material (concrete or steel) with which it is built. This observation is consistent with the UBC formula, which provide values for coefficient C for steel and concrete frames.

iv) one building, C2, was shaken with two very different acceleration levels (Table 1): the identified frequencies do differ significantly for each event, with a significant decrease (20 to 25 %, depending on the component) for the biggest event (which reached very high accelerations: 1.24 g). This is certainly an indication of non-linear behaviour, which may concern the structure itself or the soil (or both).

Based on the results, we therefore propose the following simple formula for each of the 3 building classes, and also for the "all other buildings" class:

CI:	$f_0 = 12.4 / \sqrt{H}$	or	$T_0 = 0.081 \sqrt{H}$	(8a)
CII:	$f_0 = 27.5 / H$	or	$T_0 = 0.036 H$	(8b)
S:	$f_0 = 25\,0 / H$	or	$T_0 = 0.040 H$	(8c)
CI+CS+M.	$f_0 = 52.0 / H$	or	$T_0 = 0.019 H$	(8d)

The "performances" of these formula are compared in the Table 10a with those of usual ATC and UBC formula. When keeping the H and D dependence of UBC and ATC formula, but setting free the scaling coefficient, some significant improvements are obtained, as listed in the Table 10b.

TABLE 10a: COMPARED PERFORMANCES OF UBC 88, ATC, AND THIS STUDY'S FORMULAE

Building set	σ_0	UBC formula	σ_{UBC}	ATC formula	σ_{ATC}	This study's formula	σ_3
CI	0.176	$f_0 = 20.4 / H^{0.75}$	0.190	$f_0 = 11.0 \sqrt{D} / H$	0.209	$f_0 = 12.4 / \sqrt{H}$	0.150
CII	0.304	$f_0 = 13.7 / H^{0.75}$	0.182	$f_0 = 11.0 \sqrt{D} / H$	0.437	$f_0 = 27\ 5 / H$	0.156
S	0.324	$f_0 = 11.8 / H^{0.75}$	0.101	$f_0 = 11.0 \sqrt{D} / H$	0.455	$f_0 = 25.0 / H$	0.067
CI+CS+M	0.251	$f_0 = 20.4 / H^{0.75}$	0.209	$f_0 = 11.0 \sqrt{D} / H$	0.236	$f_0 = 52.0 / H$	0.195

TABLE 10b: COMPARED PERFORMANCES OF MODIFIED UBC 88, ATC, AND THIS STUDY'S FORMULAE

Building set	σ_0	Modified UBC formula	σ_{UBC}	Modified ATC formula	σ_{ATC}	This study's formula	σ_3
CI	0.176	$f_0 = 26.4 / H^{0.75}$	0.153	$f_0 = 9.95 \sqrt{D} / H$	0.205	$f_0 = 12\ 4 / \sqrt{H}$	0 150
CII	0.304	$f_0 = 11.7 / H^{0.75}$	0.169	$f_0 = 4.34 \sqrt{D} / H$	0.167	$f_0 = 27.5 / H$	0 156
S	0.324	$f_0 = 11.5 / H^{0.75}$	0.101	$f_0 = 3.89 \sqrt{D} / H$	0.060	$f_0 = 25.0 / H$	0.067
CI+CS+M	0.251	$f_0 = 24.1 / H^{0.75}$	0.196	$f_0 = 9.71 \sqrt{D} / H$	0.213	$f_0 = 52.0 / H$	0.195

Comment: σ_0 is the logarithmic standard deviation of the data set, σ_{UBC}, σ_{ATC} and σ_3 are the logarithmic standard deviations of the differences between actual frequencies and predicted values using corresponding formulæ.

The modified ATC formula is therefore the best one for steel buildings, which is somewhat surprising, while "our" simple formula work better for all other building classes. Figure 7 shows, however, that, apart from the original ATC formula, none of the usual formula are contradicted by the present data.

IV.3 Higher mode frequencies

As shown in Table 5 to 9, it is possible to identify at least one higher mode for 21 of the 25 buildings. For almost all long period buildings (*i.e.*, those with $f_0<1$ *Hz*), the excitation level of these higher modes is very significant, as indicated by the large decrease in the residual error from

E_0 to E_1 or E_2. This is experimental proof that, at least for moderate size earthquakes (M< 6.5), careful antiseismic design of "flexible" buildings must take into account their higher modes.

It is therefore necessary to estimate the frequency of these higher modes, especially for the first harmonics. This may be done with a modal analysis, or more simply, derived from the fundamental mode frequency through a mean f_1 / f_0 ratio: from the present data set, we obtained the mean values for ratios f_1/f_0 and f_2/f_0 displayed in Table 11.

TABLE 11 AVERAGE RATIOS BETWEEN FUNDAMENTALS AND HARMONICS

Building set	First harmonics			Second harmonics		
	f_1 / f_0	Standard deviation	Number of cases	f_2 / f_0	Standard deviation	Number of cases
CI	3 36	0 76	5	-	-	0
CII	3 37	0 24	11	5 98	0 66	5
S	3 04	0 22	9	5 40	0 39	4
CS	2 56	0 42	6	-	-	0

As expected from theory for flexing or shear mode, the average f_1/f_0 ratio is slightly larger than 3; moreover, the scatter is, once again, the smallest for S and CII buildings certainly undergo a larger longitudinal to transverse mode coupling (and vice-versa). In addition, it is possible to detect, despite the scatter, a certain trend towards larger ratios for shear wall structures.

IV.4 Damping values

Despite the non-negligible uncertainty in the estimates of damping (see above section III.1), the measured values, listed in Tables 5 to 9 and displayed in Figure 8, exhibit interesting and significant features.

The main result concern the average damping $\overline{\zeta_0}$ in each building class:

Building set :	CI	CII	S	CS
$\overline{\zeta_0}$ (%) :	8.3	7.9	4.3	8.5
σ_{ζ_0} (%) :	3.8	4.4	1.7	3.7

Despite the relatively large scatter (σ_{ζ_0}) these $\overline{\zeta_0}$ values do show that damping is comparable for both shear wall and moment-resisting frame concrete buildings, and much smaller for steel buildings, thus suggesting that modal damping is correlated much more to the construction material than to the structural type.

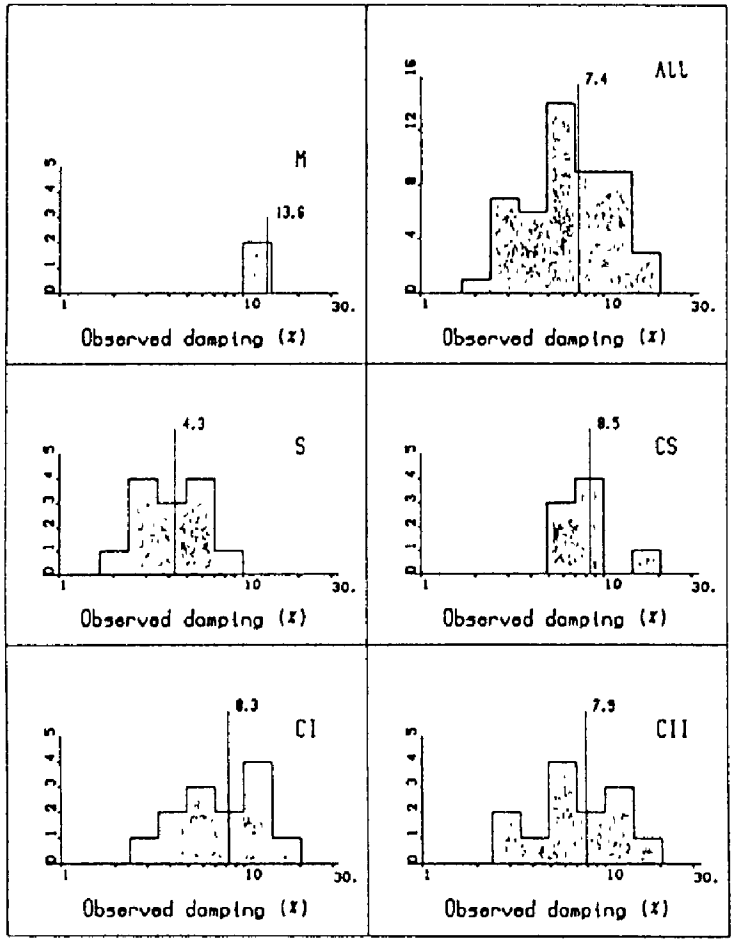

Figure 8: *Histograms of measured damping values for each building class. The damping axis is in log scale The vertical bars in each plot correspond to the average damping value for the whole building class.*

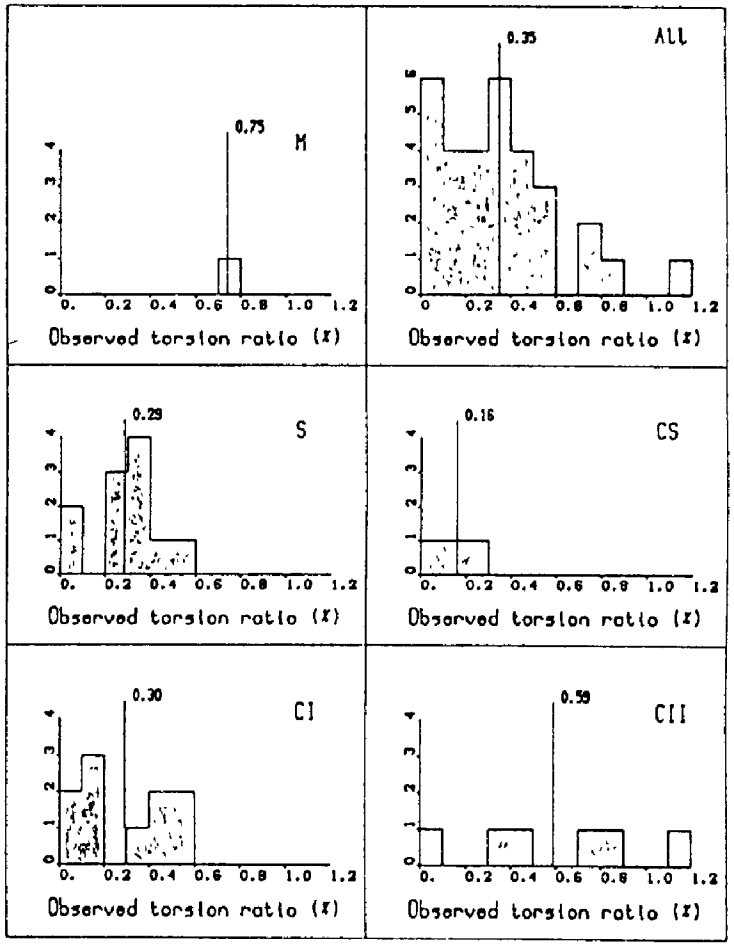

Figure 9: *Histograms of measured torsional percentage, as defined in equation (4) of text, for each building class. The vertical bars in each plot correspond to the average torsional value for the whole building class.*

The scatter in these damping values is, however, significant, and it cannot be explained by any structural (H, D,...) or input (A_{max}) parameter except, possibly, in one case: there may exist a (positive) correlation between ζ_0 and A_{max} for the CI building set. This category had already been identified, on the basis of the residual error, as the most likely to be exposed to non-linearities.

A few other observations may be derived from Tables 5 to 8:

-there is no clear correlation between the transverse and longitudinal dampings of a given building, except (possibly) for the CII and S building sets. There is, however, a trend towards a slightly larger damping in the longitudinal direction: mean ζ_L / ζ_T ratios are about 1.38 whatever the building set. There are some exceptions, *e.g.*, building C9.

-the average damping of composite buildings (CS category) is comparable to concrete buildings damping, which suggest that the actual damping of a given building is controlled by the damping of its most dissipative elements.

-it is interesting to note that the 2 damping values found for the only masonry building are amongst the largest; it is not possible to conclude, however, with so few data, that masonry is a more dissipative material than concrete (see for instance dampings of buildings C3 and C9).

-three of these 25 buildings (C6, C12 and S6) experienced two earthquakes of similar size. Although their measured natural frequencies vary only very slightly from one event to another, their measured damping does vary significantly: for the two concrete buildings, the damping increases with increasing motion level, suggesting non-linear, but reversible behaviour (the weaker event, "ML86", occurred after the stronger one, "MH84"); for the steel building, there is no such correlation, but the measured damping is certainly influenced by the amount of torsional motion, which varies considerably from one event to another (see section V). Building C2 also experienced 2 earthquakes, but with very different acceleration levels; damping and frequency values both vary as expected from classical non-linear models, but damping increase is much lower than frequency decrease: specific studies should be undertaken to understand such behaviour.

-finally, concerning the damping values for the higher modes, these are generally larger than the values obtained for the fundamental mode, and again significantly smaller for steel buildings than for concrete and composite buildings.

V. TORSIONAL MOTION

The results of the analysis described in section III.2, applied on the full set of data are summarized in Table 12, which lists both the measured amount of torsion at the fundamental transverse frequency $TR(f_0^T)$, the torsional frequency f_0^r, and the corresponding ratio $TR(f_0^r)$, with the following convention: f_0^r and $TR(f_0^r)$ are set equal to zero when $f_0^r = f_0^T$.

TABLE 12: TORSIONAL MOTION: FREQUENCIES AND AMOUNT

Building dimensions				Frequencies		"Dissymetries"			Sensor spacing	Torsional characteristics		
Id	h (m)	D1 (m)	D2 (m)	f_T (Hz)	f_L (Hz)	ς_T/ς_L	Am_T/Am_L	ψ (°)	$d/D1$	f_0^r (Hz)	$TR(f_0^r)$	$TR(f_0^T)$
C1	10.1	10.4	73.2	3.23	4.51	.72	1.50	28.	.64	3.82	1.47	.62
C2.1	20.2	21.5	22.7	4.78	3.61	2.40	1.00	53.	1.00	3.37	1.55	.35
C2.2	20.2	21.5	22.7	3.75	2.70	1.96	0.72	7.	1.00	3.00	1.00	.31
C3	16.2	33.3	41.9	2.51	1.80	.80	.52	91.	.45	.00	.00	.40
C4	21.5	24.7	62.5	2.99	5 58	.38	1.00	6.	.46	.00	.00	.51
C5	26 8	22.9	65.5	2.17	1.94	.65	.82	163.	.65	.00	.00	19
C6.1	29.3	19.4	63.9	2.35	1.61	.69	1.00	127.	1 00	00	.00	62
C6.2	29.3	19.4	63.9	2.42	1.58	1.03	1 33	81.	1.00	.00	.00	1.00
C12.1	37.8	25.0	57 9	1.62	1.09	1.65	1 00	127.	1.00	2.47	2.90	.19
C12.2	37.8	25.0	57.9	1.63	1 10	1.03	1.33	81.	1.00	2.54	1.27	.19
C7	9.1	30.5	36.6	3.39	3.71	.81	1.00	91.	1.00	3.71	2.30	1.62
C8	36.3	85.3	109.7	.70	.75	.62	.72	174.	1.00	1.06	2.17	.19
C9	20.0	19.2	46.0	.86	.97	1.94	1.21	26.	.80	.00	.00	1.79
C10	45.3	15.5	66.1	.54	1.58	.88	1.75	8.	.50	.00	.00	.71
C11	51.5	17.7	56.1	.55	.46	.60	1.22	18.	.77	.00	00	.74
C13	50.0	22.2	58.8	.40	.44	.49	.67	16.	.50	.00	.00	.34
S1	7.7	38.1	42.9	3.09	3 18	.68	.88	40	.71	.00	00	.65
S2	12.8	40.2	43.9	2.12	2 16	.73	1.00	90.	1.00	2.71	5 73	62
S3	16.0	32.6	63.7	1.79	1.79	.62	1.50	79.	.50	2.11	.78	.34
S4	25.1	36.6	36.6	.80	.78	1.69	.77	173.	1.00	1 12	.87	.13
S5	27.7	22.9	67 1	71	.89	.69	1.40	18.	.77	85	1.47	.51
S5n	27.7	22.9	37.5	.71	.89	1.00	1.40	18.	1.00	00	.00	.42
S6.1.54	64.2	50.9	50.9	.48	.48	.80	1.00	124.	.78	60	4 08	.38
S6.1.67	64.2	50.9	50.9	.48	.48	1.25	1.00	34.	.78	.58	2.91	.36
S6.2.54	64.2	50.9	50.9	.48	.50	1.69	.72	79.	.78	.59	1.62	.89
S6.2 67	64.2	50.9	50.9	.50	.48	.59	1.39	169.	.78	.60	1 88	.53
S7	82.6	32.3	32.3	.84	.86	1.17	.67	63	1.00	1.61	.51	.17
CS1	15 2	66.8	73.5	2.55	2.20	1.35	67	128.	1 00	4.30	3.20	11
CS2	29.3	92.0	137.8	3.33	3 58	.58	1 00	41	1.00	5.40	3.70	.36
CS3	28.8	14.6	18.3	1.64	1.20	1.79	1 25	1	1 00	1 87	1.47	51
M1	12.6	21 3	39 3	4.91	5.32	1.28	1.50	174.	.59	.00	.00	.88

Comments f_T (resp. f_L) is the fundamental frequency in the transverse (resp longitudinal) direction
ς_T (resp ς_L) is the damping of the fundamental transverse (resp longitudinal) mode
Am_T (resp Am_L) is the peak base acceleration in the transverse (resp longitudinal) direction.
ψ is the angle between the longitudinal axis of the building and the incoming wave

The first striking feature on this Table concerns precisely the number of cases for which fundamental transverse and torsional modes coincide: 4 out of 7 buildings of the CI class, 4/6 for CII class, 1/7 for S class, and 0/3 for CS class (a sensor malfunction in CS4 building makes upper level torsional motion unavailable). Moreover, in the remaining buildings, torsional frequency is very often only slightly different (generally larger, except in one case: C2 building, for which the first torsional mode is very clearly coupled to the first longitudinal mode) from the transverse frequency: + 15% for CI class, + 30% for CII, + 24% for S and + 48% for CS.

Another interesting result deals with the amount of torsional amount at the fundamental transverse frequency: histograms in Figure 9 displaying the "$Tor_L(f_i^T)$" values as defined in equation (4), shown that the average ratio is about 35% for the whole set of buildings, with a certain number of cases with very small torsion (10 out 31 less than 20%), but a significant number of cases with a large torsion (7 cases above 50%). The large dispersion in these values makes it a difficult to differentiate between the various building classes; steel buildings, however, exhibit rather homogeneous behaviour with a moderate though significant amount of torsion (29), while concrete frame buildings may undergo very large torsional motion (more than 70% for buildings C7, C9 and C10).

Apart from this gross differentiation however, the amount of torsion does not correlate to any of the possible "explaining" variables: neither the geometrical parameters (height, longitudinal and/or transverse dimensions), nor the structural characteristics (f_T/f_L or ς_T/ς_L ratios)

Finally, the last outstanding feature concerns the variability of the torsional motion, for the same building, from one earthquake to another: for instance, for building C6, xxxxxxx varies between 0.5 x 100 %, for C12 it does not vary at fundamental transverse frequency, but varies significantly at the torsional frequency (around 2.5 hz), for S6 it also changes substantially at both the transverse and torsional frequencies. This variability suggests that torsional motion is not a "characteristic" of the building, but is highly dependent on the incoming wavefield (azimuth, wave type, polarization,..), and that it therefore implies some kind of soil-structure interaction. In this particular data set, however, we could not point to any clear evidence for a correlation between the amount of torsional motion and the solicitation characteristics (polarization Am_T / Am_L angle ψ between the building longitudinal axis and the incoming wave, also listed in Table 12).

VI. ROCKING MOTION AND SOIL-STRUCTURE INTERACTION

Of the 25 buildings, four (i.e., C2, C6, C12 and S6) are instrumented with 2 or more vertical sensors at the base level, and are thus suited for analysis described in the section III.3. For buildings C2 and S6, which are square buildings, there are enough vertical sensors to investigate the rocking motion in both directions. Moreover, each of these 4 buildings recorded at least 2 earthquakes, as shown in Tables 1 and 2. Three out of these four buildings (C6, C12 and S6) are very "common" buildings built on "common" alluvial soils, while C2 was specially strengthened because of its particular use (telephone), and is therefore a very stiff, "nuclear-type" structure, founded on common alluvial soils.

The results are summarized in Table 13, from which the following comments may be inferred:

(i) for three of these 4 buildings, the coherence level between the rocking motion and the horizontal motion is, despite the large width of the smoothing window, extremely high (well above 0.98) at any level (roof or intermediate floors), whatever the seismic event. As for building C12, the coherence remains highly satisfactory in a 2 to 4 Hz wide frequency band centered on the fundamental mode. his result is proof of the existence of a strong soil-structure interaction for these 3 buildings.

The only building for which the coherence is poor, and therefore the soil-structure interaction weak, is the steel building, as expected: it is the most flexible ($f_0^T < 0.5\ Hz$) and it has the largest base dimensions.

(ii) for these three concrete buildings (C2, C6 and C12), the rocking motion proves to be significant to large, since it accounts for 25 to 50 % of the total horizontal motion at roof level (and for 22 to 62 % at intermediate levels). In other words, for these 3 buildings, the rocking motion represents at least one third and most 150 % of the pure flexing motion.

(iii) for the 4 buildings, the results are very consistent from one earthquake to another, since the rocking percentage remains the same (within 3 %), even though, for building C2, there exists clear non-linear behaviour which shifts the natural frequencies.

(iv) building C2 has a square foundation, but different lateral force resisting systems in the two horizontal directions: it is therefore worth nothing that, as expected, the rocking motion percentage is greater in the "stiffer" direction. Moreover, we also performed a rough estimation of the "pure" rocking periods with simple SDOF systems formula, and found exactly the same value (0.15 s) for the two directions, which is consistent with the square shape of the foundation.

(v) though the shift between fixed-base period and the period of the interacting system was not measured, some rough estimates may be derived with simple formula obtained for simple SDOF systems (such as presented in Jennings and Bielak, 1973, for instance):

$$T_0/T_f = \sqrt{1. + P},$$

where P is given by equation (5). With such a formula, the period shift is thus shown to significantly exceed 20 % in 3 (i.e., C2t, C6t, C12t) of the 6 investigated cases.

Soil-structure interaction phenomena are therefore shown to be significant to large for "common" concrete buildings built on "common" alluvial soils. As SSI is generally beneficial for structures, such a result may have significant engineering consequences for the aseismic design of many "common" buildings for which the SSI is very often disregarded. as well as for flexible buildings on very soft soils such as the Mexico City clay....

TABLE 13 : STRUCTURAL CHARACTERISTICS AND ROCKING BEHAVIOUR FOR THE 4 BUILDINGS INVESTIGATED.

Building #	Structural characteristics	Foundations Type	Foundations Soil	Frequency	Level	Height /width ratio h_n/d	Coherence level	Percentage Rocking /relative hz motion (%)	Remarks
C2	Concrete	Spread	Alluvium	4.78	Roof, mean	0.95	0.998	51	MH84, NS comp.
				3.66	Roof, mean	0.95	0 994	50	LP89, NS comp.
				3.61	Roof	0 88	0.999	26	MH84, EW comp.
				2.70	Roof	0.88	0.986	29	LP89, EW comp.
C8	RC shear-walls	Piles under	Alluvium	2 35	Roof, mean	1.60	0.987	58	MH84
				2.42	Roof, mean	1.60	0.946	56	ML86
C12	RC shear-walls	Mat	Alluvium	1 62	Roof, mean	1.72	0 997	40	MH84
				1.63	Roof, mean	1 72	0.995	36	ML86
S6	Steel frame	Mat foundation	Alluvium	0 50 0.48	Roof Roof	1.44	0.804 0.811	1 8 2.5	MH84, EW comp. ML86, EW comp
				0 48 0 48	Roof Roof	1.59	0 938 0.975	1.5 1.2	MH84, NS comp. ML86, NS comp

VII. CONCLUSIONS AND DISCUSSION

The present study is limited to a simple analysis of strong motion data, and does not address the crucial problem of the interpretation of the observed behaviour in terms of structural characteristics (and incoming wavefield characteristics): it would therefore gain substantially being coupled to a detailed structural analysis of each of these 25 buildings, so as to better appreciate the "expected" and "unexpected" parts in these observations.

On another hand, the present study should also include careful measurement of the reliability of the identified parameters. In particular, a few basic hypothesis implicit in the identification scheme should be investigated and discussed in more detail, especially the linearity hypothesis (which is obviously wrong, for instance, for C2 building, and may bias the results for concrete shear wall structures) as well as the overlook of any coupling between longitudinal and transverse motion (that the measured importance of torsional motion questions): This work is now under way, on a few characteristic examples.

However, the number of these observational measurements (25 buildings, 4 of them shaken by 2 earthquakes) allows a statistical treatment which sheds some light on the characteristics of actual behavior during real earthquakes, and therefore provides a sound data base for objective checking of computation techniques and design rules. In particular, we think that a few significant results emerge clearly enough from the data:

i) the fundamental frequency xxxx is shown to depend mainly on the building height and lateral resistance system (i.e., shear walls or frames), and not as much on construction material or horizontal dimensions. Usual ATC formula is not well suited to the observations, and thus new but simple formulae are proposed to estimate xxxx for standard buildings: their scatter is minimum for steel buildings, and maximum for concrete, shear wall buildings.

ii) damping values, though widely dispersed and less reliable than xxxx values, exhibit mean values of about 4% for steel buildings and 8% for concrete buildings. For composite buildings, modal damping is shown to be related to the most dissipative material (usually concrete).

iii) higher modes are shown to contribute significantly to the response of tall buildings, i.e. those whose fundamental period exceeds 1 s, at least for moderate size events

iv) torsional motion is shown to represent a significant (36% on average) proportion of the total relative transverse motion around the fundamental modes, even for standard symmetrical buildings, and to reach extremely large values for a few concrete frame buildings. It does not exhibit, however, any clear correlation with any geometrical or structural parameters, and it may vary a lot, for the same building, from one earthquake to another, thus suggesting great sensitivity to the incoming wavefield.

v) rocking motion is shown to be significant (i.e., 25 to 60% of the total relative transverse motion) in 3 out of the 4 cases investigated, thus showing the importance of soil-structure interaction on soft soils moderately stiff structures. In contrast to torsional motion, rocking motion is very stable from one earthquake to another.

vi) finally, steel frame buildings clearly emerge as having the simplest global behavior (i.e. with no evidence of non-linearity, minimum scatter in frequency and damping values, a reasonable amount of torsion, and minimum residual errors), while concrete, shear wall structures exhibit the most complex behaviour.

Amongst these results, we think that two them are of particular interest for the special case of Mexico City, i.e. those relating to the importance of torsional (iv) and rocking (v) motions. It has been shown (e.g., [9], [10]), that local heterogeneities in the very soft surficial clay layer are very likely to generate significant "free-field" differential motion (over 10 -3 for an event similar to the 1985 earthquake). Such differential motions, combined with the "usual" effects of the input translational motion (as shown in this paper), are thus very likely to generate very large torsional and rocking motions in medium to high rise buildings whose period is around 2 s.

We therefore think it very important to address those problems in Mexico City; in our opinion, despite the number and sophistication of existing computer codes in structural dynamics and soil-structure interaction, a sound research program should be primarily based on the dense instrumentation of a few carefully selected buildings which should also include a dense "free-field" array in the immediate vicinity of those buildings, so as to also measure the effects of soil-structure interaction on ground motion.

ACKNOWLEDGEMENTS

This work was initiated while the first author was visiting the California Division of Mines Geology in Sacramento: the help of the entire SMIP staff is gratefully acknowledged.

REFERENCES

1. Porter, L.D., J.T. Ragsdale and R.D. McJunkin, 1979. Processed data from the strong motion records of the Santa Barbara Earthquake of 13 August 1978. Final results. Special report 144, California Strong Motion Instrumentation Program., Volumes 2 and 3.

2. Huang, M. J., A. F. Shakal, D. L. Parke, R. W. Sherburne and D. V. McNutt, 1985. Processed data from the strong motion records of the Morgan Hill Earthquake of 24 April

1984. Part II: Structural response records. Report n. OSMS 85-05, California Strong Motion Instrumentation Program.

3. Shakal, A. F., M. J. Huang, C. E. Ventura, D. L. Parke, T. Q. Cao, R. W. Sherburne and R. Blazquez. CSMIP strong motion records from the Whittier, California Eartquake of 1 October 1987. Report No. OSMS 87-05, California Strong Motion Instrumentation Program.

4. Afra, H., P. Argoul et P.-Y. Bard, 1990. Identification of building structural behavior from earthquake records, Proceedings of the 9th European Conference on Earthquake Engineering, Moscow, USSR, September 11-16, 1990, vol. 7-B, pp. 3-12.

5. Beck, J., and P. C. Jennings, 1980. Structural identification using linear models and earthquake records, Earthquake Engineering and Structural Dynamics, vol. 8, pp. 145-160.

6. Luco, E., M. D. Trifunac and H. L. Wong, 1987. On the apparent change in dynamic behavior of the nine-story reinforced concrete building. Bull.seism.Soc. Am.,77, 1961-1983.

7. Bard, P.-Y., 1988. The importance of rocking in building motion: an experimental evidence. Proceedings of the 9th World Conference on Earthquake Engineering, Tokyo-Kyoto, Japan, August 2-9, 1988, Vol. VIII, p. 333-338.

8. Jennings, P., and J. Bielak, 1973. Dynamics of building-soil interaction. Bull.seis.Soc.Am., 63, 9-48.

9. Chavez-Garcia, F. J., & P.-Y. Bard, Effect of random thickness variations on the seismic response of a soft soil layer, Application to Mexico City, Engineering seismology and sute response, A.S. Cakmak and I. Herrera Editors (Proceedings of the International Conference on Soil Dynamics and Earthquake Engineering, Mexico City, October 23-26, 1989), pp. 247-261.

10. Chavez-Garcia, F. J., & P.- Y. Bard. Surface ground motion modifications by the presence of a thin resistance layer. Applications to Mexico City, Proceedings of the 9th European Conference on Earthquake Engineering, Moscow, september 1990, Vol. 4-B, pp. 37-46.